

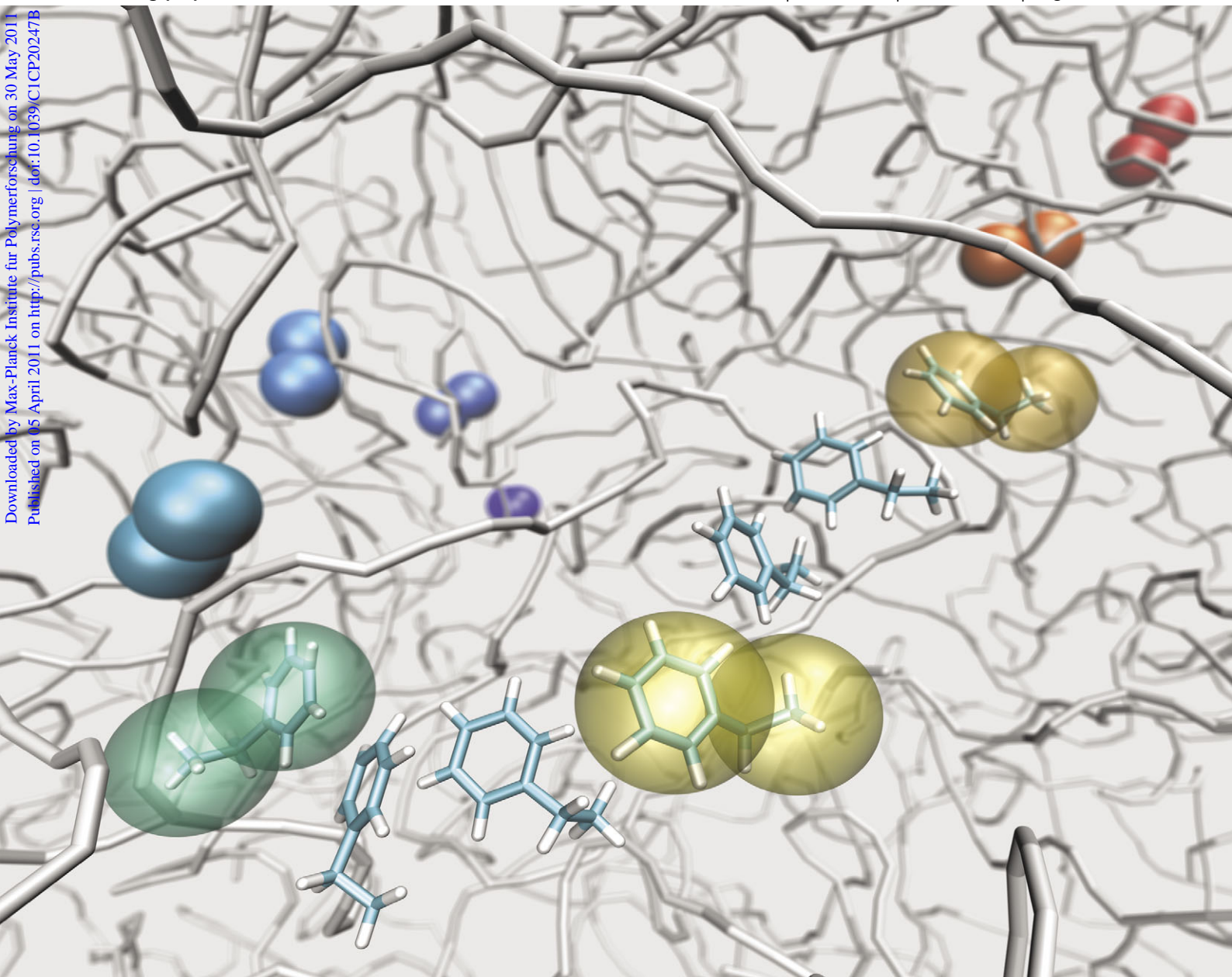
PCCP

Physical Chemistry Chemical Physics

www.rsc.org/pccp

Volume 13 | Number 22 | 14 June 2011 | Pages 10381–10824

Downloaded by Max-Planck Institute für Polymerforschung on 30 May 2011
Published on 15 April 2011 on http://pubs.rsc.org | doi:10.1039/C1CP20247B



Includes a collection of articles on the theme of multiscale modelling

ISSN 1463-9076

COVER ARTICLE

Kremer *et al.*
Multiscale modeling of soft matter:
scaling of dynamics

HOT ARTICLE

Bolhuis *et al.*
The self-assembly mechanism of fibril-
forming silk-based block copolymers



1463-9076(2011)13:22;1-Y

Cite this: *Phys. Chem. Chem. Phys.*, 2011, **13**, 10412–10420

www.rsc.org/pccp

Multiscale modeling of soft matter: scaling of dynamics†

Dominik Fritz,^a Konstantin Koschke,^a Vagelis A. Harmandaris,^{abc}
Nico F. A. van der Vegt^d and Kurt Kremer^{*a}

Received 28th January 2011, Accepted 8th March 2011

DOI: 10.1039/c1cp20247b

Many physical phenomena and properties of soft matter systems are characterized by an interplay of interactions and processes that span a wide range of length- and time scales. Computer simulation approaches require models, which cover these scales. These are typically multiscale models that combine and link different levels of resolution. In order to reach mesoscopic time- and length scales, necessary to access material properties, coarse-grained models are developed. They are based on microscopic, atomistic descriptions of systems and represent these systems on a coarser, mesoscopic level. While the connection between length scales can be established immediately, the link between the different time scales that takes into account the faster dynamics of the coarser system cannot be obtained directly. In this perspective paper we discuss methods that link the time scales in structure based multiscale models. Concepts which try to rigorously map dynamics of related models are limited to simple model systems, while the challenge in soft matter systems is the multitude of fluctuating energy barriers of comparable height. More pragmatic methods to match time scales are applied successfully to quantitatively understand and predict dynamics of one-component soft matter systems. However, there are still open questions. We point out that the link between the dynamics on different resolution levels can be affected by slight changes of the system, as for different tacticities. Furthermore, in two-component systems the dynamics of the host polymer and of additives are accelerated very differently.

1. Introduction

Properties of soft matter systems are determined by a variety of processes and interactions originating from a wide range of time and length scales. Though this holds for many physical systems, it is of special importance for soft matter, where the relevant energy scale is the thermal energy $k_{\text{B}}T$. Processes occurring on rather different scales often are governed by rather similar energy scales. As a characteristic example let us mention phase segregation effects in polymers or block copolymers. While the local dynamics on the monomer level is dominated by bond angle, torsion, and excluded volume interactions, all typically of the order of a few $k_{\text{B}}T$, the free energy difference of the whole polymer in the homogeneous mixture and the segregated state is typically also of the order

of a few $k_{\text{B}}T$. Whereas the former processes occur on a ps or at most ns time scale (if far enough away from the glass transition temperature, which we will not discuss here), the latter can take up to seconds or more if only the chains are long enough. Consequently molecular simulation approaches to soft matter phenomena require a wide range of simulation methods, which appropriately deal with different levels of resolution. Coming back to the above example, generic aspects of polymer dynamics as well as certain aspects of conformational properties like chain stiffness can be studied by highly simplified and idealized models, while specific amplitudes and prefactors, which easily can vary by orders of magnitude, or local arrangements of groups usually require detailed microscopic input. Thus a variety of different models and simulation schemes has been developed, where microscopic structure information is employed to parameterize higher level more coarse models.^{1–9} While this defines length scaling factors rigorously by the very construction, it is not at all clear how to do that for dynamical quantities in a rigorous way. Actually for most molecular systems this might be even impossible. In the following we will focus on these problems. In this context we also will discuss a more pragmatic *ansatz*, which allows us to deduce dynamical information from coarse-grained models without any adjustable parameter not coming from the simulations themselves.

^a Max-Planck-Institut für Polymerforschung, Ackermannweg 10, 55128 Mainz, Germany. E-mail: kremer@mpip-mainz.mpg.de

^b Department of Applied Mathematics, University of Crete, 71110 Heraklion, Greece

^c FORTH-IACM, 71110 Heraklion, Greece

^d Center of Smart Interfaces, Technische Universität Darmstadt, Petersenstr. 32, 64287 Darmstadt, Germany

† Electronic supplementary information (ESI) available: Technical details of the simulations presented in this work. See DOI: 10.1039/c1cp20247b

2. Scale bridging approaches

In soft matter multiscale modeling the aim is not only to describe material properties but rather to understand the structural organization and physical mechanisms, which lead to morphologies, static and dynamic properties and eventually function. That often requires multiscale models that intimately couple different levels of description, in order to span a wide range of time- and length scales. This close coupling of descriptions of different levels can be rationalized by different theoretical concepts. One way is to resort to the renormalization group theory, where the systems are also iteratively “coarse-grained”. In each renormalization step a microscopic system is mapped onto a coarser system by averaging out a number of microscopic degrees of freedom. Since the resulting coarse Hamiltonian usually cannot be determined exactly, this procedure automatically includes certain approximations. From this analogy two important aspects of common multiscale procedures emerge:

- A mapping step is always performed at a specific state point and the result might change for other state points. Thus the transferability of a given parametrization of a coarse-grained model towards different, *e.g.*, temperatures or system composition has to be checked carefully.^{10,11}

- In all practical cases the coarse-graining procedure will include unavoidable approximations. Thus the resulting coarse system usually does not follow exactly the same equation of state as the underlying microscopic system. This typically leads to pressure deviations, while correcting them then modifies the compressibility.¹²

Because of that, even though during coarse-graining only very few steps are performed, coarse-grained systems also have to be studied carefully by themselves. Structural properties are typically very well reproduced, but phase transitions or thermodynamic properties in general pose special difficulties. There is *a priori* no reason that a coarse-grained model, derived on the basis of a given scheme and some approximations, displays phase transitions at the very same temperature, pressure, *etc.* as the underlying atomistic model. In addition, the power of generic properties and scaling relations relies on the proximity to “asymptotics”, *i.e.*, chain length in the case of polymers. This often is reasonable for long chain polymer melts or chains in solution; however, many of the current systems of interest are certainly not close to the asymptotic scaling regimes.

Alternatively one can view coarse-graining procedures as a special application of projector operator formalisms.¹³ Again, the challenge is to define the optimal subspace of parameters, which allow for a most efficient treatment of the systems and, at the same time, do not exclude any aspect, which is crucial for the question under study.

Many different approaches have been followed, both from the quantum mechanical to the classical level and from the classical all-atom level to a coarse-grained description. The derivation of interaction potentials between the coarse-grained particles based on an underlying more microscopic model may be targeted at reproducing thermodynamic properties^{14–17} rather than structural properties. Such an approach, however, might cause problems, when one wants

to reproduce structural properties and especially when one wants to link local microscopic dynamics to dynamics of the more coarse-grained models. Recently Rutledge and Allen^{10,18,19} developed an alternative approach for implicit solvent models for solutions, where the excess chemical potential of the degrees of freedom, which are averaged out by coarse-graining, is properly accounted for, while simultaneously structural aspects are not neglected. Both aspects also have been considered in recent work on aggregation of amino acids and of hydrophobic solutes.^{11,20,21} In our group we predominantly employ what is called structure based coarse-graining with the aim to reproduce as close as possible on the coarse-grained level structural aspects of the underlying chemical system.^{7,9,22} Once the coarse-graining scheme is defined, the interactions are usually parameterized using the VOTCA software package developed in Mainz.²³

For the purpose of the present perspective let us assume that we have a coarse-grained model at hand, which reproduces structural properties of a polymer melt rather well and allows for a detailed comparison to experiment. Also we would like to stay that close to the all-atom description that we easily can reintroduce chemical details along the coarse-grained simulation trajectories. Such models have been developed for a number of polymers with different levels of resolutions by a number of groups.^{1,24–35} In all cases melt morphologies compare very well to, *e.g.*, scattering or NMR experiments. Fig. 1 shows two typical examples of mapping schemes for BPA-PC (polycarbonate) and PS (polystyrene). Equilibrated coarse-grained systems, for instance, then serve as a source to reintroduce atomistic details. This allows us to generate huge, well equilibrated all-atom systems, which might be used as a polymer matrix to study, *e.g.*, the tracer diffusion constant of small amounts of low molecular weight additives, a quantity very difficult to obtain from experiment.^{36–38}

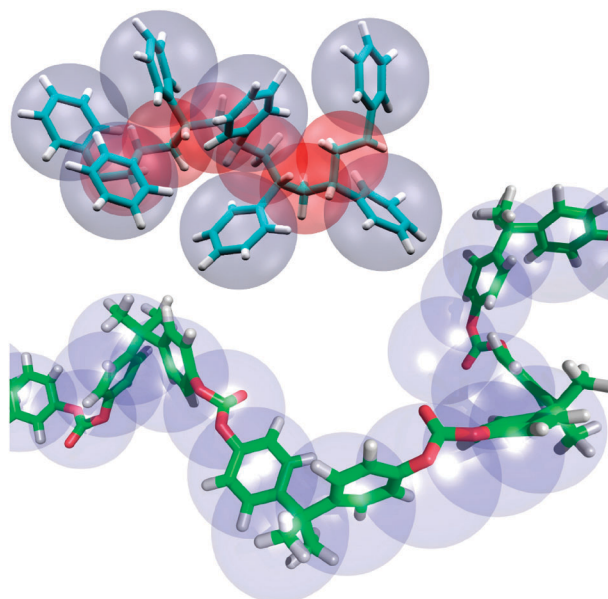


Fig. 1 Mapping schemes for PS^{33,34} (upper) and BPA-PC³⁹ (lower).

3. Scale bridging and dynamics

Coarse-grained models provide a significant simulation speedup compared to more microscopic models, which is a main reason for their application. Two possible construction schemes of coarse-grained models are illustrated in Fig. 1 for polystyrene and a polycarbonate. The representation of several microscopical particles by one coarser bead automatically determines the length scaling between the linked models, allowing for a straightforward analysis of structural properties. For dynamics, however, the link between time scales of the microscopic reference system and of the coarse system cannot be derived directly from the mapping scheme. In general, the speedup, which is not to be confused with the dynamics of the two models, results from combined effects due to the

- reduced number of degrees of freedom and simpler interaction potentials, reducing the overall computational effort
- larger integration time steps due to smoother interaction potentials
- reduced effective bead friction due to smaller energy barriers and/or a smoother energy landscape.

The first point only affects the overall computational costs, but not the dynamics itself. The second would not need further consideration, if the proper definition of the time step on the coarse-grained level with respect to the underlying microscopic model would be known. This relates to the third point, where all the problems are hidden.

- Are all barriers lowered in a way that the ratios of transition times remain the same?
- Is there a characteristic length and time scale, where an average friction coefficient describes motion/diffusion?
- Does one recover the same motion patterns for a coarse-grained simulation compared to a coarse-grained analysis of a microscopic simulation?

These are just a few questions in the context of dynamics and multiscale modeling.

For simple polymer models it is known that simulations reproduce the essential generic features of polymer dynamics, that is, the crossover from the Rouse to the entangled reptation regime for melts, qualitatively and to a certain extent quantitatively.⁴⁰ For short chains the longest relaxation time $\tau_R \propto N^2$ and for long chains in a polymer melt we observe a $N^{3.4}$ power law, N being the number of beads of the polymer. From a theoretical point of view, simple bead spring polymers are just another polymer species, for which universality holds as it does, for example, for polystyrene or polyethylene. Thus that the power laws are the same only is an indication that the simulations were performed properly. However, a rigorous link between the atomistic representation of a system and the corresponding structurally coarse-grained system could provide absolute dynamical information without the need to resort to generic scaling laws. Actually, eventually one should recover them as well. Thus one aims at a predictive quantitative modeling of dynamical quantities, such as diffusion, viscosity, rates, or correlation times. This also automatically generates the question, whether all dynamic quantities scale the same with respect to the underlying atomistic model and whether there are dependencies on molecular weight, *i.e.*, whether the

time scaling factor for an additive is the same as for the host matrix polymers.

In the case of coarse-grained models developed from chemically detailed models, as the ones discussed here, one can deduce an intrinsic simulation time scale. Taking the strength of the interaction parameter in the nonbonded excluded volume interaction (if this is described by a Lennard-Jones interaction) ϵ_{CG} (measured in units of the temperature), the average mass m_{CG} of the CG beads and the known length scales σ_{CG} one can determine a time scale $1\tau_{CG} = 1(m_{CG}\sigma_{CG}^2/\epsilon)^{1/2}$. This results for instance in $1\tau_{CG} = 1.6$ ps for BPA-PC at 570 K and $1\tau_{CG} = 1.71$ ps for atactic polystyrene at 463 K.^{39,41} Already here we have some arbitrariness in the choice of, *e.g.*, ϵ . However, since the CG interaction potentials are much smoother, barriers are lower, *etc.* the dynamics of CG systems are significantly accelerated, which eventually lead to an effective average time scaling in melts of long polymer chains of $1\tau_{\text{eff}} = 26$ ps for BPA-PC at 570 K and $1\tau_{\text{eff}} = 700$ ps for PS at 463 K, respectively, based on a comparison of mean square displacements. This discrepancy we want to focus on in the present contribution.

3.1 Basic concepts

There are several concepts, which try to rigorously map dynamics of different but related models onto each other. A typical model system is a particle moving in a cosine potential, serving as coarse-grained interaction, in comparison to a particle moving in the very same potential plus a small high-frequency modulation, representing the underlying microscopic counterpart. The aim is to find a way to predict the same diffusive dynamics. The difference in dynamics caused by the difference in potentials would therefore require to be compensated by an adjustment of the time scale. Starting with a Kramers rate picture, any crossing of barriers is related to the barrier height and the attempt frequency in the potential well. For simple systems this can be used to compare the dynamics related to rather similar potential energy landscapes.

For simulations of infrequent events Voter introduced a method for accelerating molecular dynamics simulations, called hyper-MD, already in 1997.^{42,43} The idea is based on the transition state theory, TST, which uses rates in analogy to the Kramers rate picture. The transition rate between states equals the flux through a barrier separating these states and is an equilibrium property of the system. Voter used hyper-MD to accelerate dynamics in a simulation by modifying the original potential and reestablishing the connection to the original system, in particular, to the original time scale. In this respect the idea is close to what is intended in many more recent coarse-graining methods.

TST assumes that each crossing of the dividing energy barrier is independent; therefore, all memory is lost afterwards and the next event can occur. Such a rate approach often is a good approximation to the true rates for strongly coupled systems. In hyper-MD the potential energy surface (PES) is modified in such a way that the correct relative probabilities for escapes are conserved. The potential modifications are derived from local properties of the Hessian matrix only. In more detail we will look at this method for a one dimensional

potential $V(x)$. Adding to $V(x)$ a continuous, non-negative bias boost potential $\Delta V^b(x)$, with $\Delta V^b(x) = 0$ at the dividing barrier, so that the potential is not affected close to the transition state region, leads to an effective single boosted time step

$$\Delta t_i^b = \Delta t_i^{\text{MD}} \exp[\beta \Delta V^b(x(t_i))] \quad (1)$$

and results in a total boosted time

$$t^b = \sum_i^{n_{\text{tot}}} \Delta t_i^{\text{MD}} \exp[\beta \Delta V^b(x(t_i))], \quad (2)$$

where n_{tot} is the total number of MD steps, t_i the time at the i th MD step and $\beta = \frac{1}{k_B T}$ the inverse of the temperature times the Boltzmann constant. The average boost factor is then given by

$$\frac{t^b}{t^{\text{MD}}} = \frac{1}{n_{\text{tot}}} \sum_{i=1}^{n_{\text{tot}}} \exp[\beta \Delta V^b(x(t_i))], \quad (3)$$

with $t^{\text{MD}} = n_{\text{tot}} \Delta t^{\text{MD}}$. Applying this argument to the above example of a particle moving in a cosine potential directly leads to the correct prediction of the diffusion constants. This original approach was successfully applied to the diffusion of clusters of Ag-atoms on an Ag(111) surface⁴³ and numerous variations with approximations have been developed.^{44,45} Though for typical soft matter simulations the barriers are usually of the order of a few $k_B T$, the potential energy landscape is quite complicated. Nevertheless, the guidelines to construct optimal boost potentials for hyper-MD could also serve as guidelines for other applications. The ideal bias potential should give a large boost factor, vanish at all dividing surfaces, cause a low computational overhead, avoid utilizing any prior knowledge of the dividing surfaces or the available escape paths and contain uncorrelated events only. These requirements, however, are anything but easy to fulfil. The derivation (or rather modeling) of the bias potential is the key task of hyper-MD. If successful, the simulation time can be extended by a few orders of magnitude without an increase in computer time.

A somewhat related more general approach, metadynamics, was presented by Laio and Parrinello.⁴⁶ It has been applied in a number of studies to systems with rather complicated reaction or transition pathways, especially in biophysics,⁴⁷ and has been

developed further into well-tempered metadynamics.⁴⁸ In metadynamics, potential energy basins are systematically “filled up” in order to efficiently sample transition pathways.

In all these cases the aim is to identify the optimal reaction or transition pathway, which governs the time development of the systems. Both, hyper-MD and metadynamics make use of the potential and its modifications to accelerate dynamics. With increasing number of degrees of freedom, this potential becomes very complicated and (sometimes) rough. Therefore, it is questionable, whether such methods in general can be applied to systems with many rather similar and/or permanently fluctuating energy barriers. Though conceptually rather simple, a melt of identical polymers already represents such a system. Rotations of groups around a torsion axis, for example, are not only governed by the torsion potential itself, but also by the conformation along the chain and the packing and conformations of the surrounding chains. Because of that, the bias potential ΔV^b or similar properties in other methods cannot be determined in advance and would have to be introduced on the fly.

A first rather simple polymer model, where the above ideas to a certain extent can be applied, however, is a melt of polyethylene (PE) chains. Depa and Maranas^{49,50} consider the escape of an atom from one local cage of nearest neighbors to another as an event, to which they apply the argument of the hyper-MD method. The potential energy basins on both ends of this transition arise from Lennard-Jones interactions within the spacial extent of the first shell of neighbors. The differences between the CG and the united-atom (UA) Lennard-Jones potential within this shell are forming the bias potential that causes the observed acceleration in CG dynamics. The ensemble-averaged bias potential per particle, $\langle \Delta V \rangle$, is obtained by integrating over the difference between the atomistic and the CG potential (the difference between the two is only significant throughout the first neighbor shell),

$$\langle \Delta V \rangle = \int_0^\infty \langle N_{\text{CG}}(r) \rangle U_{\text{CG}}(r) dr - \int_0^\infty \langle N_{\text{UA}}(r) \rangle U_{\text{UA}}(r) dr, \quad (4)$$

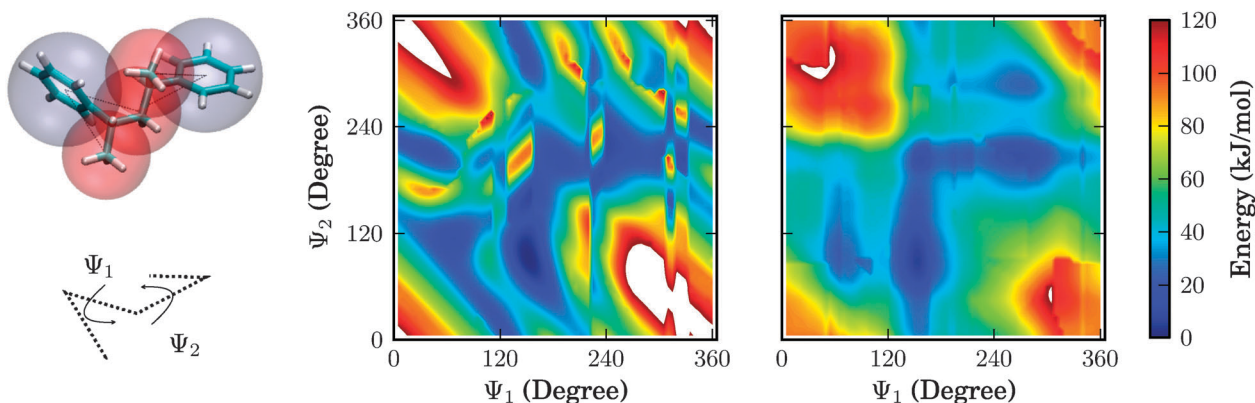


Fig. 2 Potential energy surface: potential energies for combinations of dihedral angles ψ_1 and ψ_2 in PS dimers (see left) for the atomistic (middle) and the CG model (right). In both cases one would expect a symmetric surface, but in the atomistic case the roughness of the surface illustrates the difficulties to find the atomistic conformation that realizes certain dihedral combinations with the lowest potential energy. The direction of the dihedral rotation during the extraction of the plot can still be seen.

where the CG and atomistic potentials, U_{XX} , are weighted with the ensemble-averaged number density of neighbors for each bead, $\langle N_{XX}(r) \rangle$ (XX stands for CG or UA results),

$$\langle N_{XX}(r) \rangle = \frac{\langle P_{XX}(r) \rangle}{n_{XX}} \quad (5)$$

n_{XX} is the number of particles and $\langle P_{XX}(r) \rangle$ is the averaged number density of intermolecular Lennard-Jones pairs. Similar to eqn (3), the speed-up s of the CG system is estimated by

$$s = \frac{t_{CG}}{t_{UA}} = \exp\left(\frac{\langle \Delta V \rangle}{k_B T}\right) \quad (6)$$

The predictions of this boost factor agree within 7% with simulation results for polyethylene.

The CG polyethylene system studied in their work offers certain advantages, which facilitate the application of this method. In the CG model, as well as in the united-atom model, the polymer is modeled by only one bead or atom type, *i.e.*, on both simulation levels only one type of non-bonded interaction potential has to be considered. While working for PE, already the extension to polystyrene (PS) creates insurmountable difficulties, not only due to different atom and bead types appearing on both levels, but also due to more extended side groups, where the packing between neighbors becomes more complicated. Therefore, one has to resort to a more pragmatic but still quite powerful methodology.

The more complex situation for PS already on the intramolecular level is exemplified in Fig. 2. It shows the potential energies for a PS dimer in vacuum for its different combinations of dihedral angles ψ_1 and ψ_2 , comparing the atomistic and the CG model. Even though the positions of the important minima are well defined in both cases, the atomistic potential energy surface is much more rough than the CG one. This indicates the difficulties of the atomistic model to find the energetically most favorable conformation belonging to certain combinations of dihedral angles. To extract this plot, ψ_2 was rotated stepwise by 360° for each value of ψ_1 and at each step an energy minimization from the previous conformation was performed. This directionality of the rotation can result in pathways, which only find local minima and lead to unfavorable conformations, before the system flips to conformations of lower energy. The fact that these problems occur already for the simple case of a dimer in vacuum, where only intramolecular interaction plays a role and intermolecular packing is not yet present at all, illustrates the need for a more pragmatic method to evaluate differences in atomistic and CG dynamics, which is discussed in the following.

3.2 Matching procedures relating CG and atomistic timescales

To obtain quantitative predictions of polymer dynamics from CG simulations, the timescale of the CG data has to be scaled in a suitable way to fit atomistic simulation data or experimental results. This procedure has been discussed and used in the literature before.^{1,14,24,32,33,37,38,41,49,50–52}

A suitable effective time scale τ_{eff} provides the quantitative agreement between dynamics in atomistic and CG simulations. It is obtained by comparing corresponding dynamical quantities in atomistic and CG simulations. Typical quantities

that can be chosen are diffusion coefficients and mean square displacements of beads (MSD), which are related: the self-diffusion coefficient D in a system of identical particles is calculated from the linear part of the mean square displacement of the center of mass, $\langle (R_{\text{cm}}(t) - R_{\text{cm}}(0))^2 \rangle$, as a function of time, using the Einstein relation:

$$D = \lim_{t \rightarrow \infty} \frac{\langle (R_{\text{cm}}(t) - R_{\text{cm}}(0))^2 \rangle}{6t} \quad (7)$$

The ratio between the diffusion coefficients from CG and atomistic simulations delivers the time scaling factor $s = D_{\text{CG}}/D_{\text{AA}}$. Time scaling factors based on diffusion coefficients compare only the asymptotic long time regime and require long atomistic trajectories that reach the diffusive regime. Using this quantity the CG timescale can also be mapped to experimental data.

If data from atomistic MD runs are used, the time scale τ_{eff} can be also obtained from shorter runs by matching the MSD of CG and AA simulations. Calculating the mean square displacement from CG data, $\text{MSD}(t_{\text{CG}})$, and shifting it along the time axis by a suitable time scaling factor s results in an agreement with atomistic data, $\text{MSD}(t_{\text{CG}}s) = \text{MSD}(t_{\text{CG}}\tau_{\text{eff}}/\tau_{\text{CG}}) = \text{MSD}(t_{\text{AA}})$, for times longer than t_c , a characteristic model dependent time. An example is shown in Fig. 3. This method has the advantage that the shifted MSD agrees with the atomistic MSD not only for long times, but also for times where the diffusive regime is not yet reached. This can be seen more clearly later on in Fig. 6, where the diffusion coefficient (obtained using eqn (7)) is plotted vs. inverse time. For long times D approaches asymptotically to a constant value. The agreement between CG and atomistic D or MSD is reached for times t_c long before the constant value for D is reached, in the example given in Fig. 6 for times around $t_c = 2 \times 10^3$ ps and displacements of around 0.3 nm. This provides a direct insight

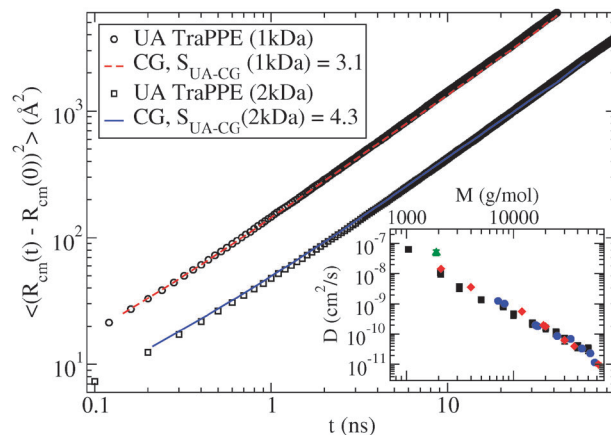


Fig. 3 Time mapping between CG and atomistic (united-atom) simulations, based on the mean square displacement of the chain center of mass for two different molecular weights of PS ($M = 1$ and 2 kDa, $T = 463$ K). In ref. 41 the time mapping was done in two steps, first relating all-atom and united-atom time scales and, secondly, united-atom and CG time scales. Inset: self-diffusion coefficient of PS melts as a function of the molecular weight from CG MD simulations (squares) and experimental data (circles,⁵³ diamonds,⁵⁴ triangle)⁵⁵ ($T = 463$ K).^{41,52}

into the time- and length scales for which the particular CG model, as illustrated in Fig. 1, can be used.

One of the simpler systems that can be studied with CG models corresponds to homogeneous one-component macromolecular systems. In general for bulk polymer systems s depends on molecular weight, M , and density, which also depends on M (chain end free volume effect). This is not surprising if we consider that the changes in the friction coefficient, and thus in the dynamics, are both due to the local polymer conformations and due to the change of the density. In contrast, at high molecular weights the change in the polymer dynamics is entirely due to the increase of the molecular weight. Because the dependence of the friction coefficient on density is not described accurately with the CG model, a dependence of s on the density and on the molecular length is resulting.

In more detail as we have seen for systems of low molecular weight s is increasing with molecular weight, but for higher molecular weights it reaches a constant value. Therefore, to describe the dynamics of long polymer chains a single value of s is appropriate (see inset of Fig. 3). It has been found that this limit of a constant scaling factor is reached for approximately the same molecular weight at which the change in density with molecular weight saturates.^{41,52} Furthermore, we have also seen that the dynamics of CG polymer melts under non-equilibrium (flowing) conditions can be described quantitatively, in a reasonable accuracy at low- to intermediate flow fields. For strong fields the predictive capabilities of the CG models would largely deteriorate.⁵⁶

Very recently, the time scaling procedure has been applied in a combined experimental and multiscale simulation approach. We have investigated the segmental and terminal dynamics of atactic PS as a function of temperature and pressure.⁵⁷ The obtained temperature dependence of relaxation times and the associated glass transition temperatures at elevated pressures investigated were found to be in good agreement with the experimentally measured glass transition temperature.

Another very important aspect concerns the effect of temperature on the dynamics of CG bulk single component polymer systems. Already in 1998 it was shown that a CG model for polycarbonates was reproducing differences in the Vogel–Fulcher (VF) behavior, which is characteristic for glass forming polymers, for different modifications of a polycarbonate.¹

Further aspects of the effective time scale are presented in the following section.

4. Specific applications and discussion: tacticity, additives

4.1 Simulation methodology

4.1.1 Atomistic simulations. For the atomistic simulations performed in this work we used an all-atom (AA) model for polystyrene (PS).⁵⁸ Details on these simulations can be found in our previous works on the influence of tacticity on static properties in polymer melts³⁴ and on the diffusion of additives in a polymer matrix of long chains³⁸ and in the ESI.†

Table 1 Atomistic systems studied in this work

$N_{\text{monomers/chain}}$	N_{chains}	$N_{\text{additives}}$	Tacticity	$\rho_{\text{AA}}/\text{kg m}^{-3}$
10	56		Atactic	959 ± 2
10	56		Isotactic	956 ± 2
10	56		Syndiotactic	959 ± 2
96	24	256	Atactic	910

All-atom PS 10-mer melts were simulated under isothermal–isobaric (NpT) conditions at a temperature of 503 K and 1 atm for atactic, isotactic, and syndiotactic tacticities. The mixed system of ethylbenzene and polystyrene was simulated under isothermal–isochoric (NVT) conditions at a temperature of 503 K and at a density of 910 kg m^{-3} , close to the experimental density. All simulated atomistic systems are listed in Table 1.

4.1.2 Coarse-grained simulations. For the coarse-grained simulations presented in this work a recently developed coarse-grained model for polystyrene was used.³⁴ The intrinsic CG time scale of this model is $1\tau_{\text{CG}} = 1.69 \text{ ps}$ at 503 K. CG simulations of pure melts were performed under isothermal–isochoric (NVT) conditions at a temperature of 503 K and at the density of the corresponding all-atomistic systems. The CG mixed system of EB and PS was simulated under isothermal–isobaric (NpT) conditions at a temperature of 503 K and 1 atm. The EB molecules in the CG simulation were modeled by the beads also used for PS and the same nonbonded potentials. All simulated CG systems are presented in Table 2.

The simulations in this work were performed with the GROMACS package⁵⁹ and the CG tools of the VOTCA package.²³

4.2 Tacticity and effective time scale

The influence of tacticity on the connection between atomistic and CG timescales is presented for PS melts with a chain length of 10 monomers. These systems are compared for three different tacticities of the PS chains. Atactic chains have random orientations of the phenyl rings along the backbone (assuming an extended all-*trans* backbone), whereas stereoregular chains have their rings all oriented in the same direction (isotactic) or in alternating directions (syndiotactic). The tacticity influences the local stiffness of the chains and by that also the overall chain dimensions in PS melts. Our CG model for PS takes the differences in local conformations into account, by using different bonded potentials for different diads. The nonbonded interactions between the CG beads are not distinguished for different tacticities.

In Fig. 4 the mean square displacement is shown for CG simulations of melts of 10-mers. The differences are small for the three different tacticities. As mentioned before, however, the timescale in these simulations is not the timescale of the underlying detailed model. To reach quantitative agreement

Table 2 CG systems studied in this work

$N_{\text{monomers/chain}}$	N_{chains}	$N_{\text{additives}}$	Tacticity	$\rho_{\text{CG}}/\text{kg m}^{-3}$
10	384		Atactic	959
10	384		Isotactic	956
10	384		Syndiotactic	959
96	24	256	Atactic	946 ± 2

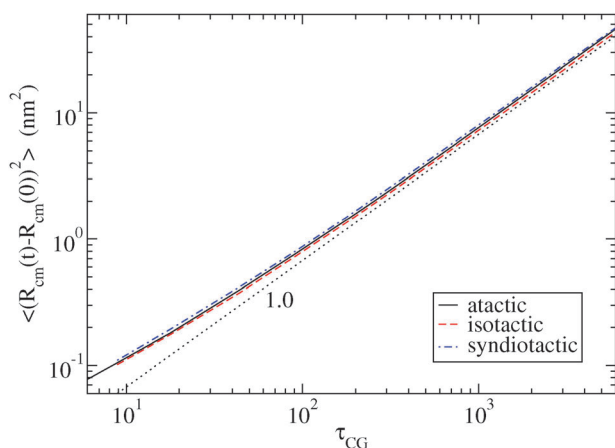


Fig. 4 Mean square displacement of coarse-grained simulations of melts of PS 10-mers of different tacticities. Results for atactic (continuous), isotactic (dashed), and syndiotactic (dashed-dotted) systems are shown as well as the slope of 1 (dotted) that indicates the diffusive regime.

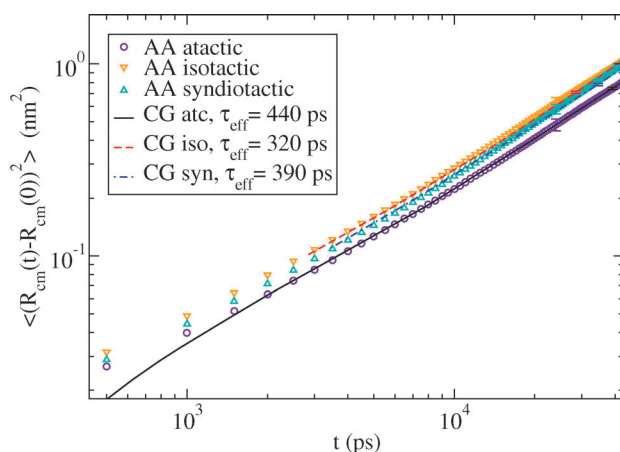


Fig. 5 Mean square displacement of atomistic and time scaled CG systems of 10-mer melts of different tacticities.

with the data of the atomistic simulations, the mean square displacement curves are shifted by adjusting τ_{eff} . This is shown in Fig. 5. The agreement between atomistic and CG MSD can be seen more clearly in Fig. 6, where the MSD is normalized by the time. The CG simulations easily reach the completely diffusive limit. Even though the atomistic data reach the diffusive regime only with large errors, the time scaling can be done in the subdiffusive regime for shorter times, where the MSD of CG and atomistic systems already coincide for times above $t_c = 2 \times 10^3$ ps.

Since the differences in the MSD are larger in the case of atomistic simulations, the effective time scales for the three tacticities are different. We obtain for the atactic system $\tau_{eff}^{atc} = 440 \pm 40$ ps, for the isotactic system $\tau_{eff}^{iso} = 320 \pm 35$ ps, and for the syndiotactic system $\tau_{eff}^{syn} = 390 \pm 35$ ps. There is no obvious connection to the chain dimensions of the three tacticities, where the syndiotactic melts show a significantly higher characteristic ratio than isotactic and atactic melts.³⁴ The possible reason for not having a unique τ_{eff} are differences in the local packing, which are reproduced by the CG model correctly, and which lead to different local frictions.

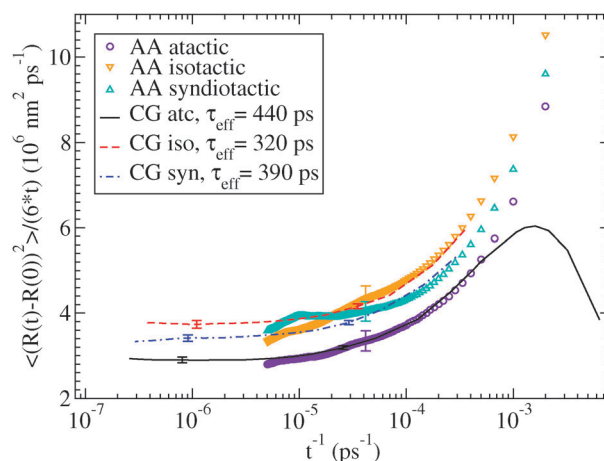


Fig. 6 MSD of atomistic and time scaled CG systems of 10-mer melts normalized by $6t$, indicating the diffusive regime reached by the CG systems and the agreement between atomistic and CG simulations, which is already reached for times above $t_c = 2 \times 10^3$ ps. The drop in the atactic CG data illustrates the transition to the ballistic regime for short times. The atomistic data have large errors for times above 10^4 ps. These long times are only shown for illustration, whereas the time scaling procedure has been done for times below 10^4 ps (see Fig. 5).

4.3 Two-component systems and effective time scales

As previously reported for polycarbonates a Vogel–Fulcher temperature dependence was found in CG simulations for the diffusion of additives in a matrix of long polystyrene chains.³⁸ Fig. 7 shows an example of the application of the time scaling procedure for diffusion coefficients for the additive ethylbenzene. In atomistic simulations at temperatures below 470 K, for which experimental data are available, it is computationally very expensive to reach the diffusive regime. CG simulations can be performed at these temperatures as well as at higher temperatures above 500 K, at which atomistic simulations are affordable. For these higher temperatures the time scaling

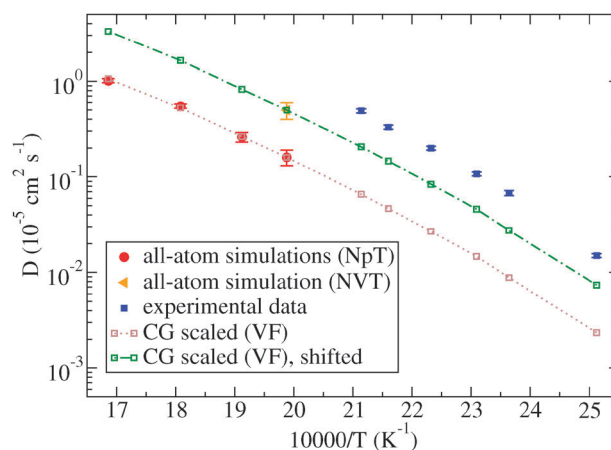


Fig. 7 Diffusion coefficients from experiments,³⁷ all-atom simulations and CG simulations. The CG data are scaled with a time scaling factor following a Vogel–Fulcher functional form. Additionally the CG data are shown with a shift, in order to coincide with the diffusion coefficient from an atomistic NVT simulation at a density close to the experimental one, because the atomistic NpT simulations predict the density 2–4% to high and therefore underestimate the diffusion coefficients.³⁸

factor $s(T)$, which is the ratio between the diffusion coefficients from CG and atomistic simulations, D_{CG}/D_{AA} , is obtained and extrapolated to lower temperatures. By that it is possible to get quantitative predictions from the CG simulations at lower temperatures. Even though the diffusion of additives is studied and not the one of the long polymer chains, the observed Vogel–Fulcher behavior reflects that the mobility of additives is linked to the structural relaxation of the polymer melt, which includes the formation and destruction of larger cavities. This process happens on much larger timescales than the local spatial fluctuations of EB in these rather rugged cavities.³⁶

Another aspect of the time scale τ_{eff} can be observed on these mixed systems of EB and PS as well: it is not only changing with temperature, but is also different for the two components EB and PS within the same system. In Fig. 8 the mean square displacements for the EB molecules and for CG beads as well as for the center of mass of the whole PS chain are shown for the all-atom (AA) simulations. The CG data are shifted to match the AA data. For EB the effective time scale is $\tau_{\text{eff}}^{\text{EB}} = 50 \pm 10$ ps, whereas the scale for the PS matrix is $\tau_{\text{eff}}^{\text{PS}} \geq 850$ ps. The time scale has to be the same for the motion of beads and for the center of mass motion, because they have the same diffusive limit. Different scaling factors for different components, even though to a smaller extent, have been also reported for CG simulations of lipid systems^{14,60} and of ionic liquids.⁶¹

It is surprising that in spite of this discrepancy the temperature dependence of the dynamics of the additive is obtained in perfect agreement with experimental results and clearly reflects the influence of the motion of the matrix of long polymer chains. An explanation might be found in the difference between the timescales on which the two components reach their diffusive regimes. To escape from a cavity formed by the surrounding chains, a trapped additive molecule does not have

to wait for a diffusive motion of the chains, but it is sufficient if beads within the surrounding chains are displaced by a distance of their bead size or even below.

5. Conclusions

Despite significant success and huge efforts by many scientists, multiscale simulations still pose many challenges. Most of the effort over the years was devoted to properly reproduce structural and in some cases thermodynamic properties. In many areas of soft matter science, but especially for amorphous polymers, this has led to a significantly improved understanding of local arrangements of polymer strands and morphological properties. Also when a very close link between the all-atom description and the more coarse view is not required or generic properties are more in the focus, simulations by now are an indispensable tool to provide (semi-)quantitative information. Here concepts of universality go in hand with the analysis of numerical data. However, already for mixtures of different species the situation is much more complicated and just now such studies, which consider chemical details of the different components, are underway. In this context the problem of transferability of interactions, derived at one state point, to another state point is of central relevance.

Even more so there are tremendous challenges when it comes to quantitative predictions of dynamical properties of materials through scale bridging simulations. For (very) long polymers universally successful concepts of polymer dynamics give important guidelines, however, provide only limited help. Also concepts like hyper-MD or metadynamics, appropriately adjusted to soft matter systems, do not really help in a system with many somewhat different and fluctuating energy barriers. The simple example of polystyrene torsion barriers illustrates this. The alternative concept of employing projection operator methodology to project out relevant dynamic degrees of freedom also requires an appropriate instantaneous knowledge and analysis of the energy landscape. Because of that, a more pragmatic approach of directly comparing short time all-atom and coarse-grained simulations provides a way out in some special situations. While this approach is quite successful for homopolymers and able to properly predict various dynamic properties including the peculiar temperature dependency of the chain dynamics without any adjustable parameter, it clearly displays its shortcomings as soon as the system becomes inhomogeneous. Despite the fact that it was possible to solidly predict additive diffusion constants in temperature regimes, where experiments are very difficult, the general scheme is unsatisfactory. The huge difference of the AA–CG time scaling factors between the host polymer and the additive clearly shows that different dynamical properties are affected by coarse-graining in a very different way. This is the central problem of time mapping during scale bridging simulations. Especially when structure formation or similar aspects are investigated a different time scaling factor for different dynamical processes almost automatically will lead to the wrong structures. As long as the different scales are very well separated, one might be able to understand the outcome and use the results of the simulations. If they are not well separated, however, this will be hardly possible. Thus the ultimate aim

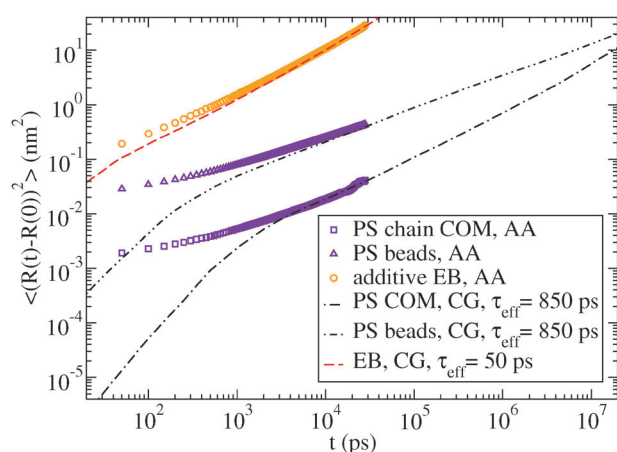


Fig. 8 Mean square displacements in mixed systems of ethylbenzene and long polystyrene chains: for ethylbenzene atomistic (circles) and CG (dashed) MSD coincide for a time scale $\tau_{\text{eff}}^{\text{EB}} = 50 \pm 10$ ps, for PS chains the atomistic center of mass of the chains (squares) and of the groups corresponding to CG beads (triangles) agree with CG data (dashed-dotted and dashed-double dotted) for $\tau_{\text{eff}}^{\text{PS}} = 850$ ps or even larger, because the atomistic data have not yet reached the diffusive regime.

would be a coarse-graining scheme, which would accelerate all dynamical processes by the same factor, while simultaneously not disturbing the general morphology. This is certainly something almost impossible to achieve, but worth the effort. In the meantime approaches as pragmatic as the ones described here might help a lot to progress our understanding of specific materials.

Acknowledgements

This work was supported by the MMM Initiative of the Max Planck Society. We thank Christine Peter, Luigi Delle Site, and Christoph Junghans for valuable discussions during the course of this work and Biswaroop Mukherjee and Victor Rühle for carefully reading the manuscript.

References

- W. Tschoep, K. Kremer, J. Batoulis, T. Bürger and O. Hahn, *Acta Polym.*, 1998, **49**, 61–74.
- J. Baschnagel, K. Binder, P. Doruker, A. A. Gusev, O. Hahn, K. Kremer, W. L. Mattice, F. Müller-Plathe, M. Murat, W. Paul, S. Santos, U. W. Suter and V. Tries, *Advances in Polymer Science: Viscoelasticity, Atomistic Models, Statistical Chemistry*, 2000, vol. 152, pp. 41–156.
- Advanced Computer Simulation Approaches for Soft Matter Sciences I*, ed. C. Holm and K. Kremer, Springer, 2005, vol. 173.
- Advanced Computer Simulation Approaches for Soft Matter Sciences II*, ed. C. Holm and K. Kremer, Springer, 2005, vol. 185.
- Advanced Computer Simulation Approaches for Soft Matter Sciences III*, ed. C. Holm and K. Kremer, Springer, 2009, vol. 221.
- Coarse-Graining of Condensed Phase and Biomolecular Systems*, ed. G. A. Voth, CRC Press, New York, 1st edn, 2009.
- M. Praprotnik, L. Delle Site and K. Kremer, *Annu. Rev. Phys. Chem.*, 2008, **59**, 545–571.
- Soft Matter*, ed. M. Wilson, 2009, vol. 5, pp. 4341–4584.
- C. Peter and K. Kremer, *Faraday Discuss.*, 2010, **144**, 9–24.
- E. C. Allen and G. C. Rutledge, *J. Chem. Phys.*, 2008, **128**, 154115.
- A. Villa, C. Peter and N. F. A. van der Vegt, *J. Chem. Theory Comput.*, 2010, **6**, 2434–2444.
- H. Wang, C. Junghans and K. Kremer, *Eur. Phys. J. E*, 2009, **28**, 221–229.
- C. Hijon, P. Espanol, E. Vanden-Eijnden and R. Delgado-Buscalioni, *Faraday Discuss.*, 2010, **144**, 301–322.
- S. J. Marrink, A. H. de Vries and A. E. Mark, *J. Phys. Chem. B*, 2004, **108**, 750–760.
- S. J. Marrink, H. J. Risselada, S. Yefimov, D. P. Tieleman and A. H. de Vries, *J. Phys. Chem. B*, 2007, **111**, 7812–7824.
- L. Monticelli, S. K. Kandasamy, X. Periole, R. G. Larson, D. P. Tieleman and S. J. Marrink, *J. Chem. Theory Comput.*, 2008, **4**, 819–834.
- R. Baron, D. Trzesniak, A. H. de Vries, A. Elsener, S. J. Marrink and W. F. van Gunsteren, *ChemPhysChem*, 2007, **8**, 452–461.
- E. C. Allen and G. C. Rutledge, *J. Chem. Phys.*, 2009, **130**, 034904.
- E. C. Allen and G. C. Rutledge, *J. Chem. Phys.*, 2009, **130**, 204903.
- A. Villa, C. Peter and N. F. A. van der Vegt, *Phys. Chem. Chem. Phys.*, 2009, **11**, 2077–2086.
- A. Villa, N. F. A. van der Vegt and C. Peter, *Phys. Chem. Chem. Phys.*, 2009, **11**, 2068–2076.
- C. Peter and K. Kremer, *Soft Matter*, 2009, **5**, 4357–4366.
- V. Rühle, C. Junghans, A. Lukyanov, K. Kremer and D. Andrienko, *J. Chem. Theory Comput.*, 2009, **5**, 3211–3223.
- W. Tschoep, K. Kremer, O. Hahn, J. Batoulis and T. Bürger, *Acta Polym.*, 1998, **49**, 75–79.
- H. Fukunaga, J. Takimoto and M. Doi, *J. Chem. Phys.*, 2002, **116**, 8183–8190.
- J. Padding and W. J. Briels, *J. Chem. Phys.*, 2002, **117**, 925–943.
- G. Milano and F. Müller-Plathe, *J. Phys. Chem. B*, 2005, **109**, 18609–18619.
- Q. Sun and R. Faller, *Macromolecules*, 2006, **39**, 812–820.
- H. Qian, P. Carbone, X. Chen, H. A. K. Varzaneh, C. C. Liew and F. Müller-Plathe, *Macromolecules*, 2008, **41**, 9919–9929.
- P. Carbone, H. A. Karimi-Varzaneh, X. Chen and F. Müller-Plathe, *J. Chem. Phys.*, 2008, **128**, 064904.
- H. A. Karimi-Varzaneh, P. Carbone and F. Müller-Plathe, *J. Chem. Phys.*, 2008, **129**, 154904.
- V. A. Harmandaris, N. P. Adhikari, N. F. A. van der Vegt and K. Kremer, *Macromolecules*, 2006, **39**, 6708–6719.
- V. A. Harmandaris, D. Reith, N. F. A. van der Vegt and K. Kremer, *Macromol. Chem. Phys.*, 2007, **208**, 2109–2120.
- D. Fritz, V. A. Harmandaris, K. Kremer and N. F. A. van der Vegt, *Macromolecules*, 2009, **42**, 7579–7588.
- G. Rossi, L. Monticelli, S. R. Puisto, I. Vattulainen and T. Ala-Nissila, *Soft Matter*, 2011, **7**, 698–708.
- O. Hahn, D. A. Mooney, F. Müller-Plathe and K. Kremer, *J. Chem. Phys.*, 1999, **111**, 6061–6068.
- V. A. Harmandaris, N. P. Adhikari, N. F. A. van der Vegt, K. Kremer, B. A. Mann, R. Voelkl, H. Weiss and C. C. Liew, *Macromolecules*, 2007, **40**, 7026–7035.
- D. Fritz, C. R. Herbers, K. Kremer and N. F. A. van der Vegt, *Soft Matter*, 2009, **5**, 4556–4563.
- S. Leon, N. F. A. van der Vegt, L. Delle Site and K. Kremer, *Macromolecules*, 2005, **38**, 8078–8092.
- K. Kremer, *Simulations in Condensed Matter: From Materials to Chemical Biology*, Springer, 2006, vol. 704.
- V. A. Harmandaris and K. Kremer, *Macromolecules*, 2009, **42**, 791–802.
- A. F. Voter, *J. Chem. Phys.*, 1997, **106**, 4665–4677.
- A. F. Voter, *Phys. Rev. Lett.*, 1997, **78**, 3908–3911.
- C. Sanz-Navarro and R. Smith, *Comput. Phys. Commun.*, 2001, **137**, 206–221.
- X. G. Gong and J. W. Wilkins, *Phys. Rev. B: Condens. Matter*, 1999, **59**, 54–57.
- A. Laio and M. Parrinello, *Proc. Natl. Acad. Sci. U. S. A.*, 2002, **99**, 12562–12566.
- A. Laio and F. L. Gervasio, *Rep. Prog. Phys.*, 2008, **71**, 126601.
- A. Barducci, G. Bussi and M. Parrinello, *Phys. Rev. Lett.*, 2008, **100**, 020603.
- P. K. Depa and J. K. Maranas, *J. Chem. Phys.*, 2005, **123**, 094901.
- P. K. Depa and J. K. Maranas, *J. Chem. Phys.*, 2007, **126**, 054903.
- B. Hess, S. Leon, N. F. A. van der Vegt and K. Kremer, *Soft Matter*, 2006, **2**, 409–414.
- V. A. Harmandaris and K. Kremer, *Soft Matter*, 2009, **5**, 3920–3926.
- M. Antonietti, K. J. Fölsch and H. Sillescu, *Makromol. Chem.*, 1987, **188**, 2317–2324.
- G. Fleischer, *Colloid Polym. Sci.*, 1987, **265**, 89–95.
- O. Urakawa, S. F. Swallen, M. D. Ediger and E. D. von Meerwall, *Macromolecules*, 2004, **37**, 1558–1564.
- C. Baig and V. A. Harmandaris, *Macromolecules*, 2010, **43**, 3156–3160.
- V. A. Harmandaris, G. Floudas and K. Kremer, *Macromolecules*, 2011, **44**, 393–402.
- F. Müller-Plathe, *Macromolecules*, 1996, **29**, 4782–4791.
- B. Hess, C. Kutzner, D. van der Spoel and E. Lindahl, *J. Chem. Theory Comput.*, 2008, **4**, 435–447.
- L. Thøgersen, B. Schiøtt, T. Vosegaard, N. C. Nielsen and E. Tajkhorshid, *Biophys. J.*, 2008, **95**, 4337–4347.
- H. A. Karimi-Varzaneh, F. Müller-Plathe, S. Balasubramanian and P. Carbone, *Phys. Chem. Chem. Phys.*, 2010, **12**, 4714–4724.